Mucin 1 downregulation decreases the anti-tumor effects of melanoma vaccine

Fangfang Shi[1,2], Rui Xue[1], Hui Xu[1], Feng Mei[1], Xueyang Bao[1], Jun Dou[1], Fengshu Zhao[1]

[1]Department of Pathogenic Biology and Immunology, School of Medicine, Southeast University, Nanjing, China; [2]Department of Oncology, Zhongda Hospital, School of Medicine, Southeast University, Nanjing, China

Contributions: (I) Conception and design: F Shi, R Xue, H Xu, J Dou, F Zhao; (II) Administrative support: J Dou, F Zhao; (III) Provision of study materials or patients: J Dou, F Zhao; (IV) Collection and assembly of data: R Xue, F Mei, X Bao; (V) Data analysis and interpretation: F Shi, R Xue; (VI) Manuscript writing: All authors; (VII) Final approval of manuscript: All authors.

Correspondence to: Fengshu Zhao; Jun Dou. Department of Pathogenic Biology and Immunology, School of Medicine, Southeast University, 87 Ding Jiaqiao Road, Nanjing 210009, China. Email: Fengshu_zhao@126.com; njdoujun@seu.edu.cn.

Background: Immunotherapy-based approaches are important breakthroughs with potential treatment benefits for melanoma patients. Mucin 1 (MUC1) is significantly upregulated in melanoma relative to normal cells. It has been reported that MUC1 influences cancer cell proliferation, apoptosis, invasion, and metastasis. The study aimed to explore the effect of *MUC1* knockdown on the biological characteristics of the melanoma cell line B16F10 and evaluate whether MUC1 is an effective candidate target antigen for melanoma vaccine development.

Methods: First, lentiviral vector-mediated short hairpin RNA (shRNA) was used to knockdown *MUC1* in B16F10 cells (sh*MUC1*-B16F10 cells). Next, we examined epithelial-mesenchymal transition (EMT), migration, proliferative capacity, clone formation, and distribution of cell cycle in shMUC1-B16F10 cells. Finally, the vaccine was prepared by repeated freeze-thawing of the sh*MUC1*-B16F10 cells and used to subcutaneously immunize C57BL/6 mice, which were then challenged using B16F10 cells 10 days after the final vaccination.

Results: It was revealed that sh*MUC1* suppressed B16F10 proliferative and colony formation capacity, induced the arrest of cell cycle in the G0/G1 phase, and adjusted the expression of EMT-associated factors. MUC1 downregulation markedly suppressed the effect of B16F10 vaccine against melanoma in a mouse model. As compared with B16F10-vaccinated mice, B16F10-vaccinated mice in which *MUC1* was silenced had reduced natural killer (NK) cytotoxicity, lower production of interferon-γ (IFN-γ), anti-MUC1 antibodies, perforin, granzyme B, and elevated tumor growth factor-β (TGF-β) level.

Conclusions: MUC1 has strong melanoma vaccine immunogenicity, and induces the host's anti-tumor reaction. *MUC1* knockdown inhibits the immune activity of B16F10 cell vaccine and anti-melanoma effect, suggesting the MUC1 is an important candidate target antigen of the melanoma vaccine.

Keywords: Melanoma; melanoma vaccine; mucin 1 (MUC1); target antigen; vaccination

Submitted Nov 07, 2022. Accepted for publication Dec 13, 2022.
doi: 10.21037/atm-22-6170
View this article at: https://dx.doi.org/10.21037/atm-22-6170

Introduction

Melanoma, a fatal malignancy that originates from melanocytes, accounts for about 80% of skin cancer-related deaths, although it comprises only 5% of skin cancers. Localized melanoma is mainly treated through surgery, which is not effective in metastatic disease (1). Although chemotherapy improves melanoma prognosis, the median survival time of metastatic melanoma is no more than 10 months, and the surviving rate is merely 27% (2). Previously, important immune checkpoint inhibitors

(ICIs) acting on programmed cell death-ligand 1 (PD-L1), programmed cell death-1 (PD-1), and cytotoxic T-lymphocyte-associated protein 4 (CTLA-4), were reported to be effective treatments for melanoma treatment (3-5). However, a significant proportion of patients still do not benefit from these treatments or develop secondary resistance to the drugs (6). In the past 30 years, the efficacy for metastatic melanoma treatments has remained low despite extensive research.

Unlike prophylactic vaccines, tumor vaccines are therapeutic and are designed to break the immune system's tolerance to cancer antigens. Tumor vaccines provoke immune responses to specific tumor-associated antigens by activating $CD8^+$ and $CD4^+$ T cells (7,8). Therefore, it is crucial to find candidate antigens that may enhance the efficacy of melanoma vaccines. The current research team has previously sought to develop melanoma vaccines (9,10). Our previous findings, as well as those of other groups, have indicated that tumor vaccines can inhibit and kill tumor cells by activating specific cytotoxic T lymphocyte (CTL) effects and by inducing the production of specific antibodies in tumor-bearing hosts. However, due to the diminished immunogenicity in tumor cells and the complexity of cancer immune escape, there is a wide gap between actual tumor vaccine benefits and expected outcomes. Researchers have taken keen interest in identifying highly efficient, specific, and strongly immunogenic antigens that may enhance the efficiency of melanoma vaccines.

Normally, secretory epithelial cells express mucin 1 (MUC1) on the surface membrane. Its differential expression in normal versus cancer cells makes it a promising antigen for cancer immunotherapy (11,12). Over 80% of human cancers are MUC1-positive (11,12). The current research group has confirmed that the MUC1 expressed in mouse colon tumor cells has a dominant antigenic epitope that elicits MUC1 antibody production (13). MUC1's immunogenicity is associated with the epitopes of B cell receptor and T cell receptor, and it has potential as a vaccine antigen candidate (14). Modulation of MUC1 expression affects the immunogenicity of anticancer vaccines and their antitumor effects. In normal cells, large amounts of MUC1 sugar chains prevent the presentation of antigenic peptides and hinder the proximity of CTLs, thereby avoiding the killing of autologous cells by CTLs (14-16). However, MUC1 has emerged as a novel glycopeptide epitope due to its configuration change, loss of steric hindrance in tumor cells, and easy exposure to immune cells. Additionally, epithelial-mesenchymal transition (EMT) and cancer metastasis can be promoted by MUC1 overexpression. The co-transportation of the C-terminal transmembrane subunit of MUC1 into the nucleus along with β-catenin may suppress E-cadherin as well as upregulate Snail, Slug, vimentin, and Twist. It was also found that the PD-1 and PD-L1 expressed highly in MUC1-positive colon cancer cells, which suggested that there was the positive correlation between the expressions MUC1 and PD-1. It is very promising to apply immunotherapy for targeting the PD-L1/PD-1 signaling pathway in MUC1-positive cancer (14-16). Our previous report showed that the immunogenicity of colon cancer vaccines significantly correlates with MUC1 expression level (13).

Here, *MUC1* was silenced in murine melanoma B16F10 cells using short hairpin RNA (shRNA). sh*MUC1*-B16F10 and B16F10 cell vaccines were then prepared using the repeat freeze-thawing approach and their anti-tumor efficacy examined. The data from the study show that MUC1 is a key target antigen for melanoma, and that downregulating MUC1 reduced a clonal formation, proliferation, and migration capabilities of B16F10 cells *in vitro* and weakened the immunogenicity and anti-tumor effects of the sh*MUC1*-B16F10 vaccine when compared with the B16F10 vaccine *in vivo* in C57BL/6 mice. Altogether, these findings imply that MUC1 mediates the anti-tumor efficacy of the melanoma B16F10 cell vaccine. The data offers valuable support for clinical research on melanoma vaccination. We present the following article in accordance with the ARRIVE reporting checklist (available

Highlight box

Key findings

- MUC 1 downregulation decreases the anti-tumor effects of melanoma vaccine.

What is known and what is new?

- MUC1 influences cancer cell proliferation, apoptosis, invasion, and metastasis.
- MUC1 knockdown inhibits the immune activity of B16F10 cell vaccine and anti-melanoma effect, suggesting the MUC1 is an important candidate target antigen of the melanoma vaccine.

What is the implication, and what should change now?

- It highlights MUC1 as an important dominant target antigen and offers novel insights into melanoma vaccine development.

Table 1 Primer sequences for RT-qPCR analysis

Gene	Forward (5'-3')	Reverses (5'-3')
GAPDH	CAGCTACTCGCGGCTTTACG	GTGATGGGCTTCCCGTTGAT
MUC1	ACGTGAAGTCACAGCTTATACA	AGGGCAAGGAAATAGACGATAG
E-cadherin	GAGTGCCACCACCAAAGACA	GAAAACATTGGTTGAGATAAGCCT
N-cadherin	TCTCCTAACCCAGGGCCTTA	CACCGCTACTGGAGGAGTTG
Vimentin	CTAGCCGCAGCCTCTATTCC	AAGCGCACCTTGTCGATGTA
Perforin	CCTCCTATGGCACGCACTTTATC	TCCACGTTCAGGCAGTCTCCTAC
Granzyme B	AGATCTCCTGCTACTGCTGACC	GCTGCTGATCCTTGATAGAAAGT

RT-qPCR, real time quantitative polymerase chain reaction; GAPDH, glyceraldehyde-3-phosphate dehydrogenase; MUC1, mucin 1.

at https://atm.amegroups.com/article/view/10.21037/atm-22-6170/rc).

Methods

Cell culture

Murine melanoma cells, B16F10, and human renal epithelial cells, HEK 293T were purchased from Shanghai Academy of Biological Sciences (Shanghai, China). The mouse lymphoma cell line, YAC-1, was obtained from the Chinese Academy of Sciences cell bank (Shanghai, China). The B16F10 and YAC-1 cell lines were passaged in Roswell Park Memorial Institute (RPMI) 1640 complete medium enriched with 1% mixture of penicillin-streptomycin and 10% fetal bovine serum (FBS; Gibco, Waltham, MA, USA). The HEK 293T cell line was grown in Dulbecco's modified Eagle medium (DMEM) enriched with 1% mixture of penicillin-streptomycin and 10% FBS (17). The passaging of cells was performed at conditions of 37 ℃, 5% CO_2, and in a humidified incubator. The morphology of cells was observed under an inverted microscope.

Construction of a B16F10 cell line with stable silencing of MUC1

A stable *MUC1*-silenced B16F10 cell line (shMUC1 B16F10) was constructed as described previously (18). Briefly, the B16F10 cell line was cultured with 5×10^4 cells per well in 24-well plates, until the cells reached 50–70% confluence. Those cells were then transfected by replacing the normal culture media with diluted sh*MUC1* lentiviral stock solution. After 72 hours, the B16F10 cells were digested with trypsin, and then washed with phosphate-buffered saline (PBS). After that, they were seeded on 10 cm-culture dishes (Sigma-Aldrich, St. Louis, MO, USA), with 500 cells per dish, followed by continuous selection using puromycin (Thermo Scientific, Cleveland, OH, USA) for 3 weeks. We selected clones that survived with cloning rings. This was followed by expansion and subcloning procedures based on the limiting dilution method. The efficiency of *MUC1* silencing was then determined through western blotting and real-time quantitative polymerase chain reaction (RT-qPCR) tests.

Western blot and RT-qPCR analyses

Next, the efficiency of *MUC*1 silencing was evaluated in the stably-infected cells (Lv-sh*MUC1*-B16F10) relative to cells transfected with scramble shRNA and wild type B16F10 cells. We used RT-qPCR to determine the *MUC1* messenger RNA (mRNA) and different EMT factors, *N-cadherin*, *E-cadherin*, and *vimentin*, using Vazyme ChamQ™ SYBR qPCR master mix (Low ROX Premixed) (Code: Q331-02/03; Vazyme, Nanjing, China) as described before (19,20). Step One Plus™ real time system (Applied Biosystems, Framingham, MA, USA) was used to apply RT-qPCR. The cycling conditions were as follows: in stage 1, the initial heat activation was performed at 95 ℃ for 3 minutes. Then, the denaturation was applied at 95 ℃ for 10 seconds. Finally, the combined annealing/extension process was conducted for 40 cycles, at 60 ℃ for 30 seconds (18). The ΔΔCt method was applied to calculate relative gene expression, with glyceraldehyde-3-phosphate dehydrogenase (GAPDH) as reference gene. Primers used are presented in *Table 1*.

To determine MUC1 protein expression level, 2×10^6 Lv-sh*MUC1*-B16F10 cells, scramble cells, and wild type

B16F10 cells were separately lysed with an extraction buffer for proteins (78501, Thermo Scientific, USA). Western blot analysis was conducted as previously described (21,22) using MUC1 recombinant rabbit monoclonal antibody (1:1,000, ab45167, Abcam, Cambridge, UK), horseradish peroxidase (HRP)-conjugated goat anti-rabbit IgG (H + L, 1:2,000, ab205718, Abcam), and rabbit anti-GAPDH antibody (1:10,000, ab8245, Abcam) (18).

Determination of proliferation and colony formation ability of cells

Colony formation and Cell Counting Kit-8 (CCK-8) assays were conducted as described previously (13,18). Briefly, about 200 B16F10 cells, scramble cells, and Lv-sh*MUC1*-B16F10 cells were seeded in 6-well plates (NEST Biotechnology, Wuxi, China). When the cell colonies had formed 14 days later, 0.1% solution of crystal violet (Sigma-Aldrich) was used to stain them at room temperature for 30 minutes in the dark. Excess dye solution in the stained plates was removed by washing 3 times using PBS. After air drying the above plates, the clones were counted, and the data were analyzed statistically using GraphPad (GraphPad Software, San Diego, CA, USA).

For CCK-8 cell proliferation assays, 2×10^3 B16F10 cells, scramble cells, or Lv-sh*MUC1*-B16F10 cells per well were added into 96-well plates. Then, 3 wells from each group were then incubated for 4 hours with 10 µL of CCK-8 (Sigma-Aldrich) per well, every day. The optical density (OD) of each cell solution was recorded under 450 nm wavelength in the microplate reader (Perkin-Elmer, Waltham, MA, USA) followed by data analysis on GraphPad. Cell proliferation rate (%) = (OD of various days – 0 h OD)/(0 h OD – blank control OD) × 100%.

Cell cycle analysis

About 1×10^6 cells (B16F10, scramble, or Lv-sh*MUC1*-B16F10) were harvested and rinsed with PBS as described previously (23). Cells were added to 500 µL of ice-cold buffer, centrifuged, and the supernatant was discarded. They were then rinsed in PBS after 30 minutes of fixing using cold ethanol at 4 ℃. Next, they were resuspended in 500 µL RNase A (100 µg/mL, KeyGEN, Nanjing, China) and incubated at 37 ℃. After 30 minutes, 200 µL propidium iodide (PI) staining solution (50 µg/mL) was used to resuspend and incubate those cells on ice for 30 minutes in the dark. Finally, the cell cycle distribution in each group was analyzed through a flow cytometry (FCM) machine [Becton, Dickinson, and Co. (BD), Franklin Lakes, NJ, USA].

Migration assay

Transwell migration assay was conducted as described previously (13). Briefly, 3×10^4 cells (B16F10 cells, scramble cells, or Lv-sh*MUC1*-B16F10 cells) were added into the upper transwell chambers (Corning, Inc., New York, NY, USA) and cultured for 36 hours. Then, the cells in those chambers were dyed with 0.1% solution of crystal violet (Sigma-Aldrich) after fixation. They were then imaged (magnification: 200×) on 6 random fields of view per chamber and data analyzed on GraphPad 8 software.

Vaccine preparation

Vaccine preparation was conducted as previously reported (13,18). Briefly, whole tumor cell lysate vaccines were prepared using the repeat freeze-thaw method by 30 minutes of freezing 5×10^6 cells (B16F10 cells, scramble cells, or Lv-sh*MUC1*-B16F10 cells) at –80 ℃ followed by 30 minutes of thawing at room temperature. This process was repeated thrice.

Experimental protocol in vivo

To estimate the anti-tumor efficiency of the Lv-sh*MUC1*-B16F10 vaccine *in vivo*, 60 C57BL/6 mice (female, age: 5–6 weeks, weight: 16–18 g) purchased from the Animal Center of Yang Zhou University of China were housed under specific-pathogen-free (SPF) conditions and routinely raised. Male C57BL/6 mice are easy to fight with each other in the same cages, resulting in injury or death. Given the long duration of the experiment, to avoid the additional interference caused by the above conditions on the experimental results, we chose relatively mild female C57BL/6 mice. Experiments were performed under a project license (No. 20200405010) granted by the animal research and ethics board of Southeast University, in compliance with Chinese Ethics Committee guidelines for the care and use of animals. A protocol was prepared before the study without registration. Mice were divided randomly into the PBS, B16F10, scramble, and Lv-sh*MUC1*-B16F10 vaccination groups (n=5 in each group). All the C57BL/6 mice were administered subcutaneous

immunization 3 times (an interval of 10 days between the vaccinations), with various indicated vaccines (density: 5×10^5) on the right side of abdomen. The mice were continued to be fed for 10 days following the final time of vaccination. Then, 2×10^6 B16F10 cells were administered in the back subcutaneously. The tumor growth of the mice in various groups was examined and recorded dynamically once every 5 days. The calculation formula (length multiplied by the square of the width divided by 2) was used to determine tumor volumes (mm^3). This was repeated thrice and analyzed on GraphPad 8.0 software.

Cytotoxicity assays

Cytotoxicity assays were conducted as described previously (13,18). In summary, splenocytes were collected from vaccinated mice 18 days after being challenged with B16F10 and depleted of erythrocytes by the lysis buffer (Beyotime Biotechnology, Shanghai, China). The collected splenocytes were resuspended with RPMI 1640 medium with 15% FBS for further use. YAC-1 and B16F10 cells were collected, marked with the 5,6-carboxyfluorescein diacetate succinimidyl ester (CFSE; 20 μg/mL) (Invitrogen, Carlsbad, CA, USA) at 37 ℃ for 30 minutes and then washed with cold PBS. To estimate the cytotoxicity of natural killer (NK) cells, NK effector cells were cultured in Corning U-bottom 96 well plates (3×10^6 cells per well), then were incubated with YAC-1 target cells (1×10^5 cells per well) for 6 hours at 37 °C in a cell culture incubator. For the antibody-dependent cell-mediated cytotoxicity (ADCC) assay, a total of 1×10^5 B16F10 target cells were incubated with 3×10^6 effector splenocytes in a medium containing serum from vaccinated mice at a 30:1 ratio at 37 ℃ for 6 hours. After incubation, the different effector-target cells were harvested and rinsed with pre-chilled PBS 3 times. Finally, all the cell samples were labeled with 7-AAD (Beyotime Biotechnology) at room temperature for 10 minutes and detected using FCM (BD), followed by analysis on FlowJo X (BD).

Enzyme-linked immunosorbent assays (ELISAs)

About 18 days after the cells were challenged with B16F10, immunized sera were collected from mice in vaccine groups. The corresponding ELISA kits and HRP-labeled antibodies were then prepared to determine the levels of tumor growth factor-β1 (TGF-β1), interferon-γ (IFN-γ), and the titers of anti-MUC1 immunoglobulin G (IgG) antibody in the sera, according to manufacturer instructions (eBioscience, Vienna, Austria). Briefly, sera samples were diluted at a ratio of 1:5, and each cytokine was captured by the specific primary monoclonal antibody and detected by biotin-labeled secondary antibody. Plates were read at 450 nm using a microplate reader (Perkin-Elmer). Samples and standards were run in triplicate, and the sensitivity of the assays was 0.1 U/mL for IFN-γ and TGF-β1. Sera samples were diluted at 1:10 for detecting anti-MUC1 IgG antibody (13,18).

RT-qPCR analysis

The tumor tissues from the mice in various vaccine groups were shredded, ground, and fully lysed on ice for the extraction of total RNA using the corresponding extraction kit (Vazyme Biotech, China, RM201-01). Then, RT-qPCR was conducted as previously described to determine the mRNA expression levels of *E-cadherin*, *vimentin*, *N-cadherin*, *perforin*, as well as *granzyme B* (13,18).

Statistical analysis

All the data were pooled and analyzed with GraphPad Prism 8 software. The data were from at least three independent experiments. Group differences were compared with the Student's *t*-test and expressed as mean ± standard deviation (SD). A P value less than 0.05 was chosen as the threshold for statistical significance.

Results

MUC1 plays a pivotal role in B16F10 biological characteristics

To investigate if MUC1 affects biological characteristics of B16F10 cells, the stable sh*MUC1* B16F10 cell line was developed. Significant downregulation of *MUC1* expression in LV-sh*MUC1*-B16F10 cells was observed, as shown in *Figure 1*. *MUC1* knockdown markedly reduced the proliferation of B16F10 cells. The number of clones and the rate of cell proliferation in the Lv-sh*MUC1*-B16F10 group were lower than in the B16F10 and scramble groups (*Figure 2*). The percentage of cells arrested in G0/G1 stage in the Lv-sh*MUC1*-B16F10 group was elevated when compared with the B16F10 and scramble groups (*Figure 3*). The ratio of cells arrested in S stage was even less in the Lv-sh*MUC1*-B16F10 group than in either

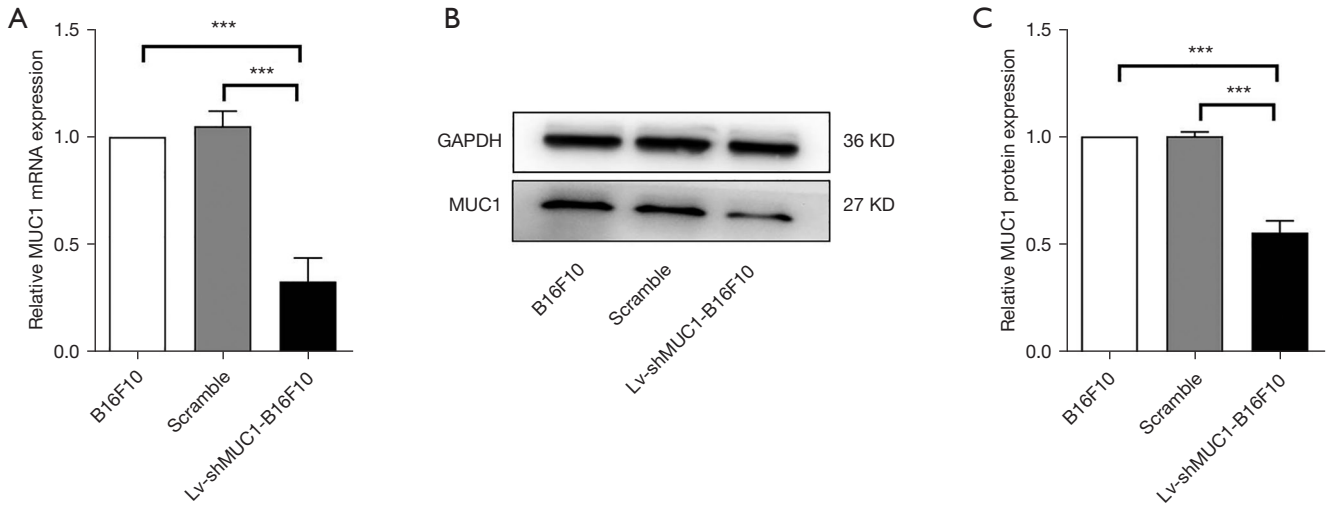

Figure 1 Detection of *MUC1* expression in B16F10 cells, scramble cells, and Lv-sh*MUC1*-B16F10 cells. (A) *MUC1* expression was tested in various cells separately by RT-qPCR. (B,C) *MUC1* expression was tested in various cells by western blotting. ***P<0.001. *MUC1*, mucin 1; mRNA, messenger RNA; sh*MUC1*, short hairpin *MUC1*; GAPDH, glyceraldehyde-3-phosphate dehydrogenase; RT-qPCR, real time quantitative polymerase chain reaction.

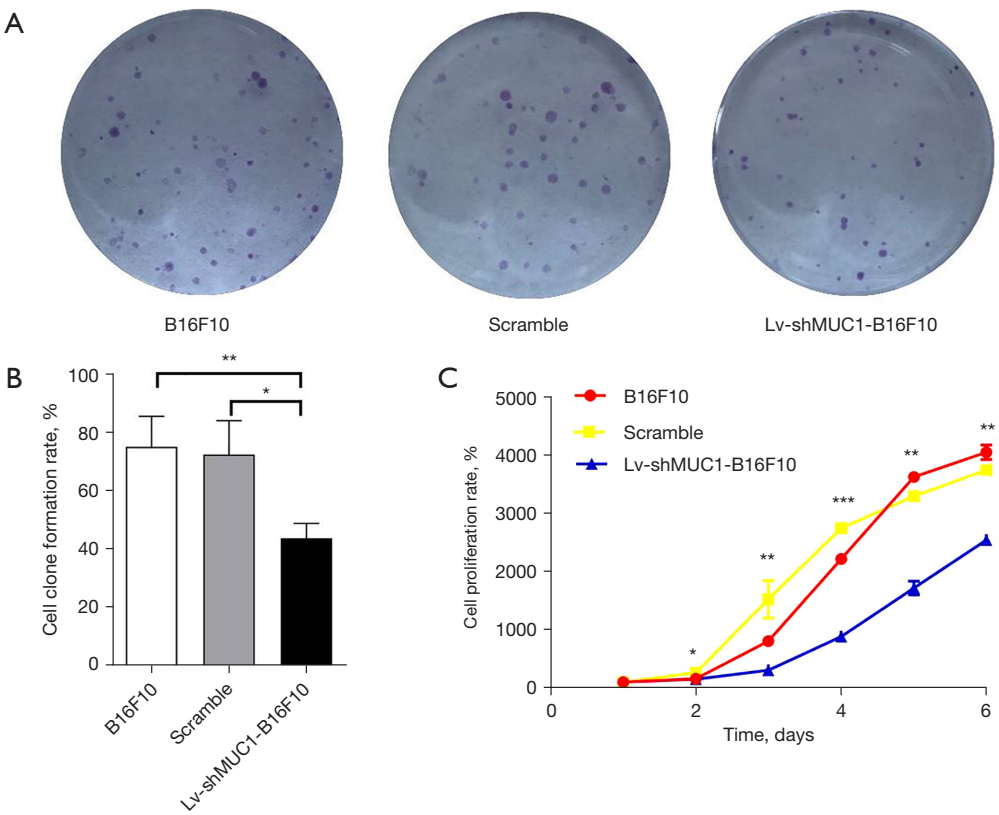

Figure 2 The effects of *MUC1* knockdown on cell proliferation. (A) The number of clones in B16F10 cells, scramble cells and Lv-sh*MUC1*-B16F10 cells stained with 0.1% crystal violet (magnification: 100×). (B) Various cell clone formation rate was measured in plate with crystal violet stain assay. (C) The proliferation rate was determined in various cells by CCK-8 assay. *P<0.05; **P<0.01; ***P<0.001. *MUC1*, mucin 1; sh*MUC1*, short hairpin *MUC1*; CCK-8, Cell Counting Kit-8.

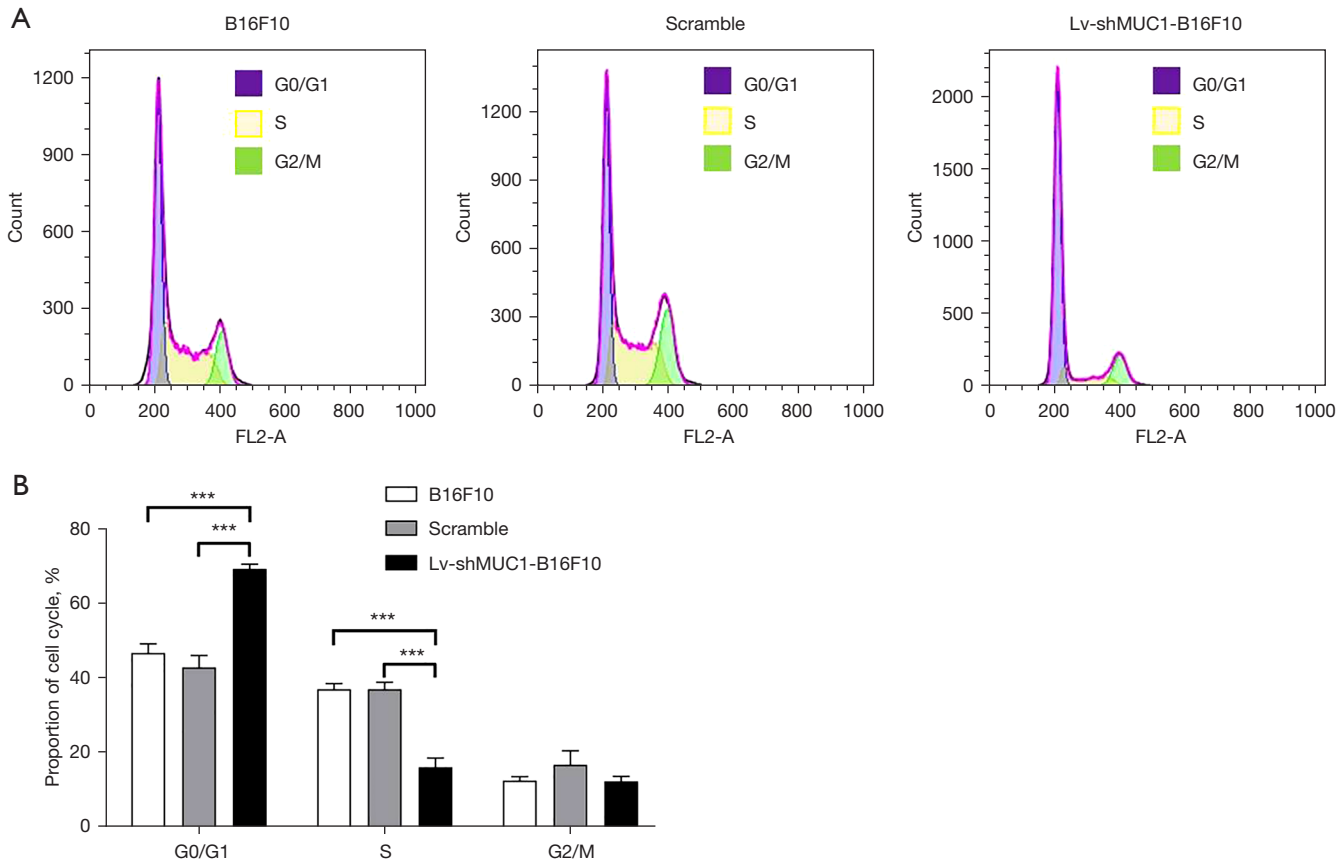

Figure 3 The effects of *MUC1* knockdown on cell cycles. (A) The cell cycle distribution in B16F10 cells, scramble cells and Lv-sh*MUC1*-B16F10 cells was analyzed by FCM. (B) The proportion of cells in various cell cycle stages. ***P<0.001. *MUC1*, mucin 1; sh*MUC1*, short hairpin *MUC 1*; FCM, flow cytometry.

B16F10 group or scramble group (*Figure 3*). These findings indicate that *MUC1* downregulation induced the cycle arrest of B16F10 cells in G0/G1 phase. To explore whether MUC1 impacted the migration of B16F10 cells, transwell assay was conducted. This analysis revealed that fewer cells migrated in the Lv-sh*MUC1*-B16F10 group than in either the B16F10 group or scramble group (*Figure 4*), indicating that *MUC1* knockdown inhibits the migration of B16F10 cells. Moreover, it was found that the mRNA level of *E-cadherin* was elevated (*Figure 5A*), whereas that of *vimentin* and *N-cadherin* was markedly decreased in the Lv-sh*MUC1*-B16F10 group when compared with the B16F10 and scramble groups (*Figure 5B,5C*). In general, the above results show that MUC1 plays an extremely important biological role in B16F10 cells.

MUC1 is needed for the B16F10 vaccine to exhibit tumor-inhibitory effects

To assess if *MUC1* knockdown affects the effectiveness of the B16F10 vaccine, all the mice were subcutaneously immunized 3 times in the right flank using various vaccines (5×10^5 cell lysates) at 10-day intervals between the vaccinations. At an interval of 10 days from the last vaccination, about 2×10^6 B16F10 cells were administered subcutaneously in the C57BL/6 mice (*Figure 6A*). The experiment was repeated independently 3 times with 5 mice in each group. Notably, the B16F10 cell vaccine significantly inhibited tumor growth when compared with PBS. However, tumor mass in mice administrated with the Lv-sh*MUC1*-B16F10 vaccine were much larger when

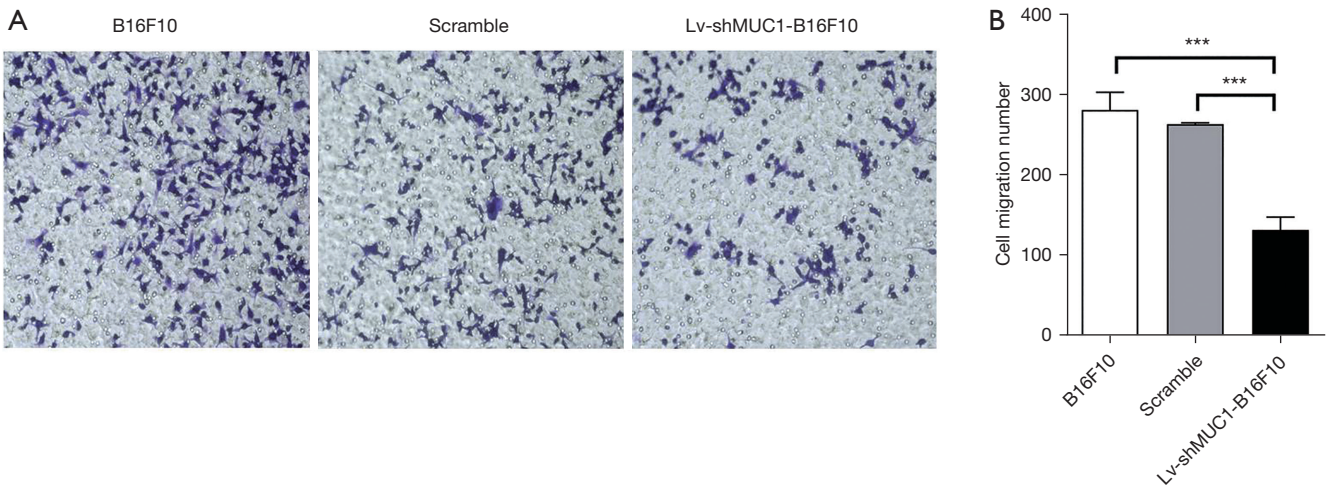

Figure 4 The influence of *MUC1* knockdown on cell migration. (A) Cell migration in B16F10 cells, scramble cells, and Lv-sh*MUC1*-B16F10 cells was analyzed by transwell migration assay. Migrated cells were stained with 0.1% crystal violet (magnification: 200×). (B) Cell migration number in various cells. ***P<0.001. *MUC1*, mucin 1; sh*MUC1*, short hairpin *MUC1*.

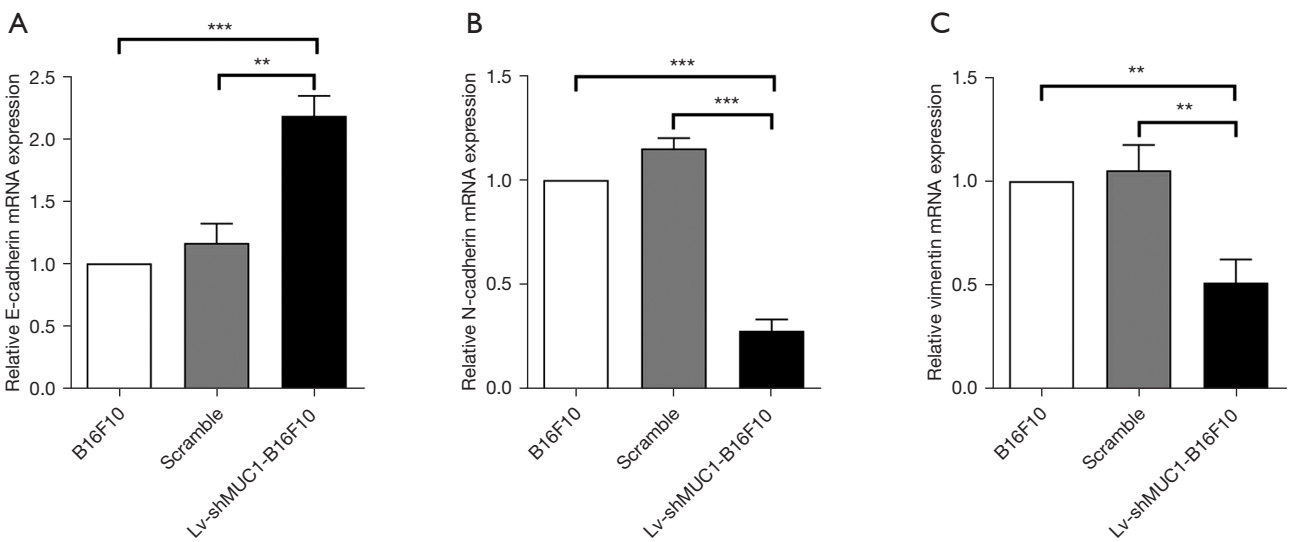

Figure 5 Detection of cell mRNA levels of invasion related proteins. (A) The mRNA level of *E-cadherin* in B16F10 cells, scramble cells and Lv-sh*MUC1*-B16F10 cells. (B) The mRNA level of *N-cadherin* in various cells. (C) The mRNA level of *vimentin* in various cells. All the mRNA expression levels in various cells were analyzed by RT-qPCR. **P<0.01; ***P<0.001. mRNA, messenger RNA; *MUC1*, mucin 1; sh*MUC1*, short hairpin *MUC1*; RT-qPCR, real time quantitative polymerase chain reaction.

compared to mice inoculated with the B16F10 vaccine or scramble vaccine (*Figure 6B*,*6C*). Of note, *MUC1* knockdown blunted the efficacy of the B16F10 vaccine in suppressing tumor growth (*Figure 6B*,*6C*), suggesting that MUC1 may mediate the immunogenicity of B16F10 vaccine. Moreover, the B16F10 vaccine markedly delayed tumorigenesis in vaccinated mice when compared with PBS; the Lv-sh*MUC1*-B16F10 vaccine exhibited a worse effect of delaying tumorigenesis than the B16F10 and scramble vaccines (*Figure 6D*). The prophylactic efficacy of the Lv-sh*MUC1*-B16F10 vaccine was poorer than those of B16F10 and scramble vaccines (*Figure 6D*). Importantly, *MUC1* silencing reduced the protection of the B16F10 vaccine against challenge with B16F10 cells (*Figure 6B-6D*).

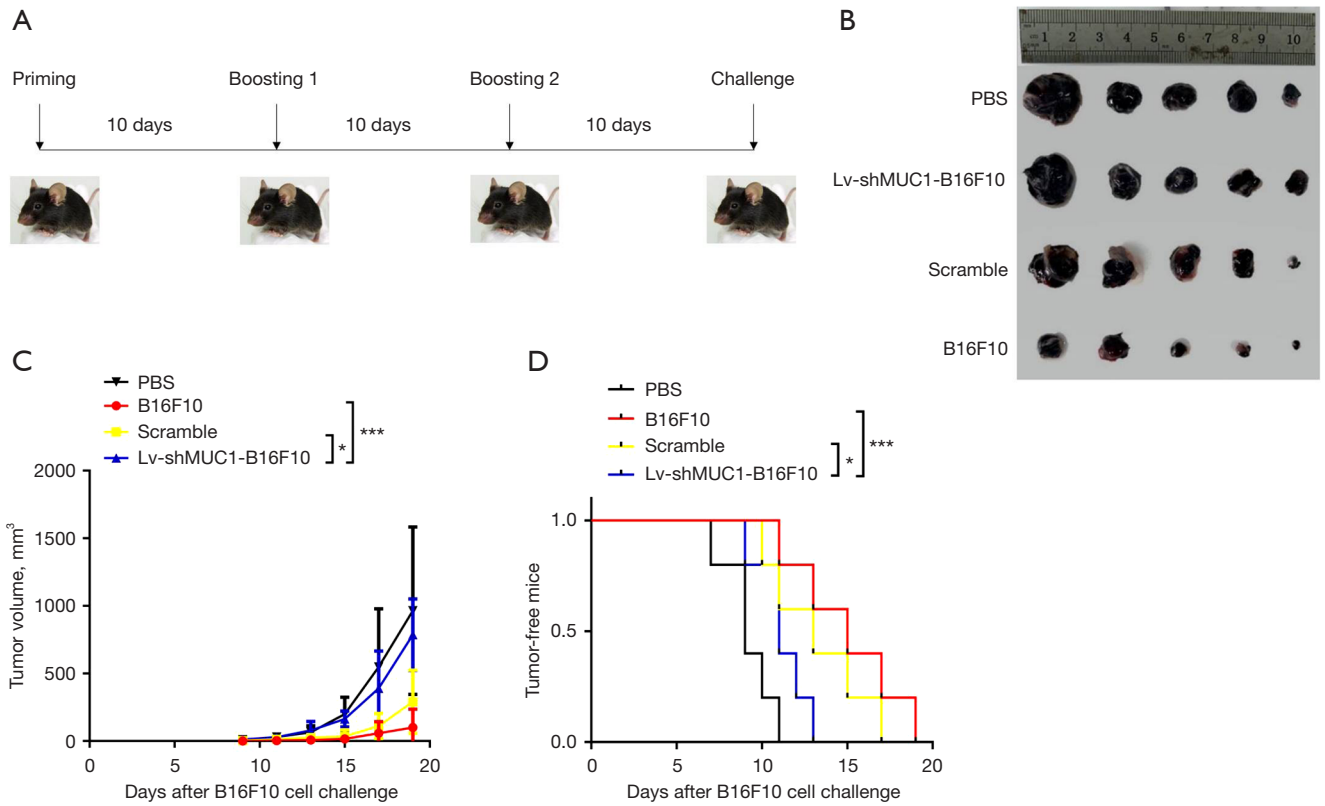

Figure 6 The influence of *MUC1* knockdown on tumor growth in vaccinated mice. (A) The immunization strategy used in the study *in vivo*. (B) Tumor mass at 18 days after B16F10 challenge in B16F10 tumor-bearing mice that were first vaccinated 3 times at 10-day intervals with various inactivated vaccines (5×10^5), then challenged using B16F10 cells (2×10^6) 10 days after the final vaccination. (C) The tumor volume was dynamically recorded in various vaccine groups. (D) Tumor-free time was monitored throughout the experiment. *P<0.05; ***P<0.001. PBS, phosphate-buffered saline; *MUC1*, mucin 1; sh*MUC1*, short hairpin *MUC1*.

Since EMT is a key player in melanoma pathogenesis, the mRNA levels got next evaluated of different EMT factors, *vimentin*, *N-cadherin*, and *E-cadherin* in tumor tissues from multiple groups using RT-qPCR. This analysis showed that *E-cadherin* mRNA level was remarkably decreased in the Lv-sh*MUC1*-B16F10 vaccine group than in either B16F10 group or scramble vaccine group, but higher than in the PBS group (*Figure 7A*). The mRNA levels of both *vimentin* and *N-cadherin* were significantly enhanced in the Lv-sh*MUC1*-B16F10 vaccine group than in the B16F10 and scramble vaccine groups, but decreased than in the PBS group (*Figure 7B*,*7C*). Altogether, these results indicate that *MUC1* knockdown blunted the anti-tumor efficiency of the B16F10 vaccine.

Down-regulation of MUC1 attenuated the conferred effect of the B16F10 vaccine on the cytolytic activity of NK cells

To explore whether down-regulation of *MUC1* affected the cytotoxic immunocyte responses following B16F10 vaccine inoculation, the cytotoxicity of NK cells was first investigated in the vaccinated C57BL/6 mice. The result indicated that the cytotoxic responses of NK cells were increased in the Lv-sh*MUC1*-B16F10 vaccine group when compared to the PBS group, but significantly reduced compared with the B16F10 and scramble vaccine groups (*Figure 8A*,*8B*). Next, analysis of ADCC activity revealed that it was markedly impaired in the Lv-sh*MUC1*-B16F10

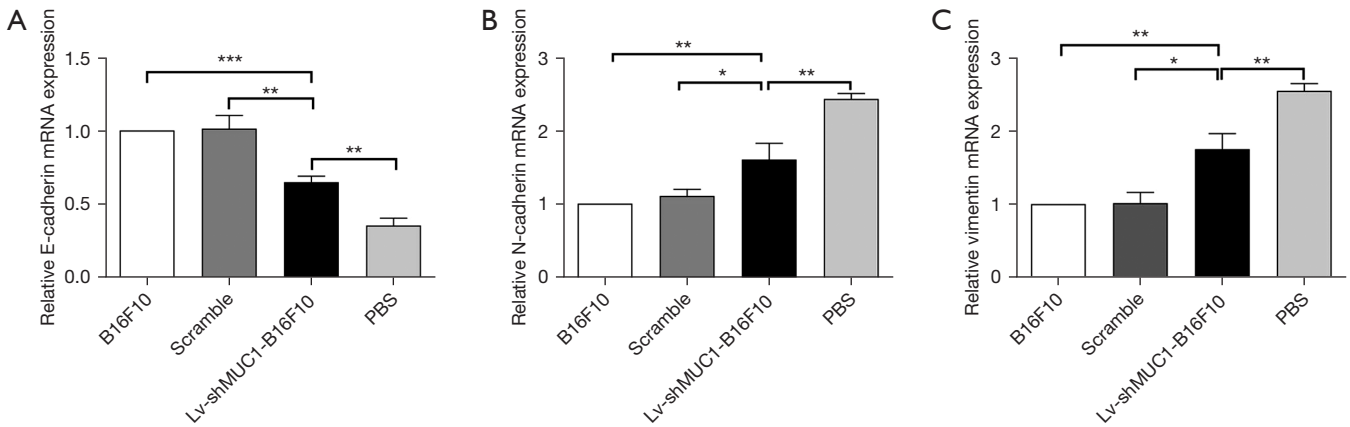

Figure 7 Detection of mRNA levels of invasion related proteins in tumor tissues. (A) Tumor mRNA level of *E-cadherin* in B16F10 group, scramble group, Lv-sh*MUC1*-B16F10 group and PBS group. (B) Tumor mRNA level of *N-cadherin* in different groups. (C) Tumor mRNA level of *vimentin*. All the mRNA expression levels in various tumor tissues were quantified using RT-qPCR. *P<0.05; **P<0.01; ***P<0.001. mRNA, messenger RNA; *MUC1*, mucin 1; sh*MUC1*, short hairpin *MUC1*; PBS, phosphate-buffered saline; RT-qPCR, real time quantitative polymerase chain reaction.

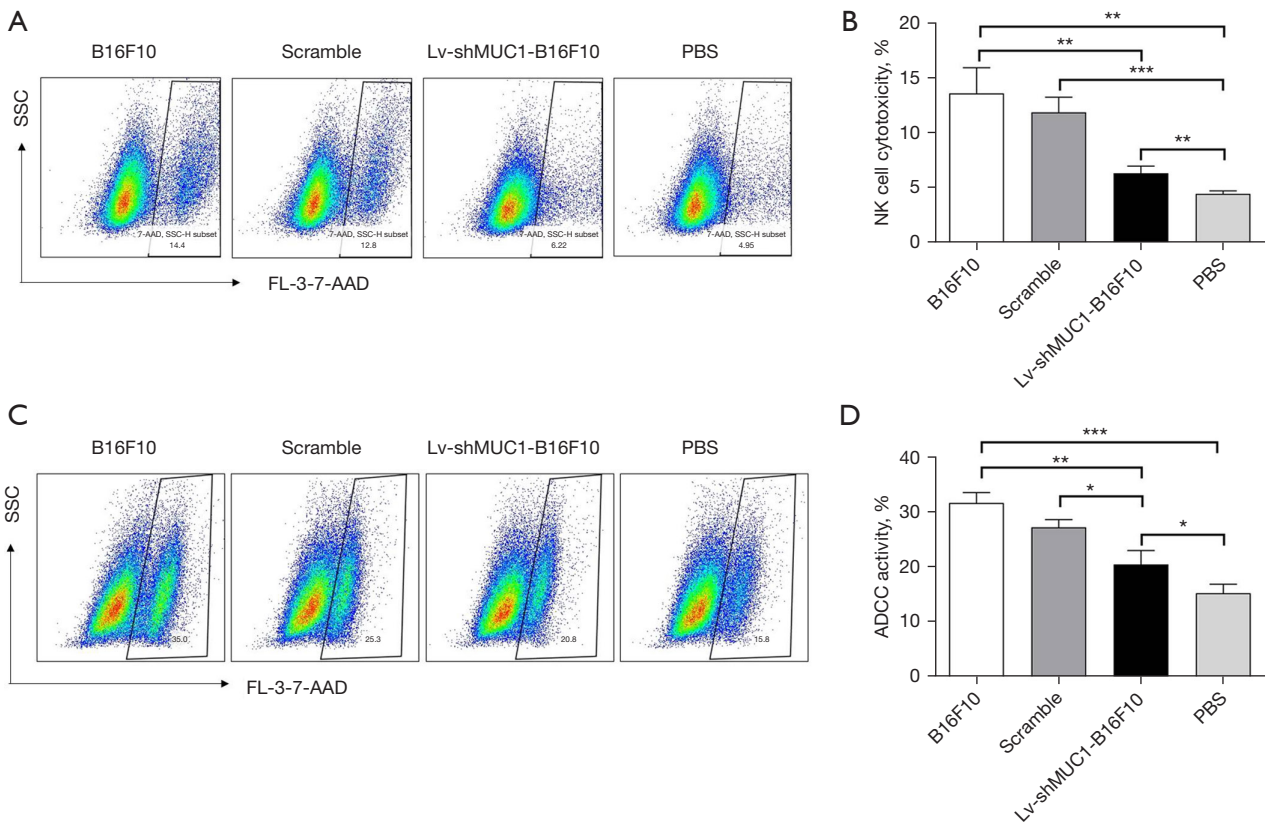

Figure 8 Knocking down *MUC1* impaired the proficiency of the B16F10 vaccine to induce cytotoxicity in NK cells. (A) The cytotoxicity of NK cells (target: YAC-1 cells) was detected using FCM in various vaccine groups. (B) The statistical analysis result of NK cytotoxicity, referring to the differences as indicated. (C) ADCC activity (target: B16F10 cells) was detected using FCM in various vaccine groups. (D) The statistical analysis result of ADCC activity, referring to the differences as indicated. *P<0.05; **P<0.01; ***P<0.001. SSC, side scatter; *MUC1*, mucin 1; sh*MUC1*, short hairpin *MUC1*; PBS, phosphate-buffered saline; NK, natural killer; ADCC, antibody dependent cell-mediated cytotoxicity; FCM, flow cytometry.

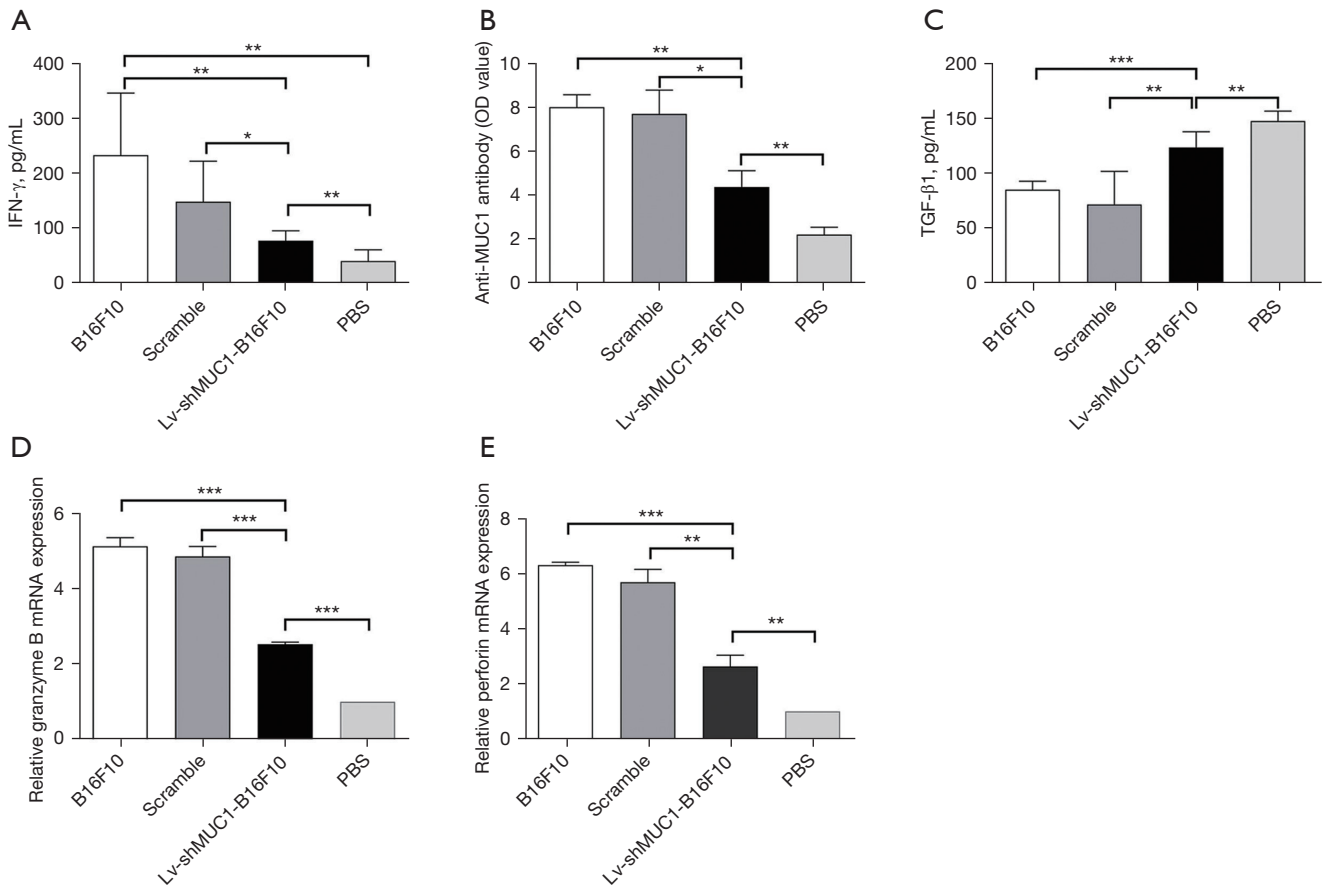

Figure 9 Detection of the inflammatory factors and antibody production in vaccinated mice. (A-C) Serum IFN-γ, anti-MUC1 antibody, and TGF-β1 levels were evaluated using ELISA in different groups. (D,E) RT-qPCR analysis of the levels of *granzyme B* and *perforin* in tumor tissues from vaccinated mice. *P<0.05; **P<0.01; ***P<0.001. IFN-γ, interferon-γ; *MUC1*, mucin 1; sh*MUC1*, short hairpin *MUC1*; TGF-β, tumor growth factor-β; OD, optical density; mRNA, messenger RNA; ELISA, enzyme linked immunosorbent assay; RT-qPCR, real time quantitative polymerase chain reaction.

vaccine group compared with the B16F10 and scramble vaccine groups but was higher than in the PBS group (*Figure 8C*,*8D*). Knocking-down *MUC1* significantly decreased the effect of the B16F10 vaccine on enhancing ADCC activity. Of all vaccine groups, B16F10 cell vaccine triggered the highest cytolytic capacity in immune cells.

MUC1 knockdown impaired the immunoreaction induced by B16F10 vaccine in vaccinated mice

Next, analysis of the effect of knocking down *MUC1* on the release of TGF-β1 and IFN-γ, as well as the production of anti-MUC1 IgG antibody in the sera of vaccinated mice revealed lower serum concentration of IFN-γ and anti-MUC1 IgG antibody in the Lv-sh*MUC1*-B16F10 vaccine group than those of the B16F10 and scramble vaccine groups (*Figure 9A*,*9B*). Moreover, the Lv-sh*MUC1*-B16F10 vaccine notably enhanced the TGF-β1 level in serum when compared with the B16F10 and scramble vaccines (*Figure 9C*). Additionally, the mRNA expression of both *perforin* and *granzyme B* in tumor tissues was decreased in the Lv-sh*MUC1*-B16F10 vaccine group in contrast to the B16F10 and scramble vaccine groups (*Figure 9D*,*9E*). These results indicate that knocking down *MUC1* weakened the activity of the B16F10 vaccine in inducing the production of anti-MUC1 antibody and the expression of granzyme B, perforin, and IFN-γ, but enhanced the TGF-β1 secretion in serum from the mice that were immunized using the Lv-sh*MUC1*-B16F10 vaccine.

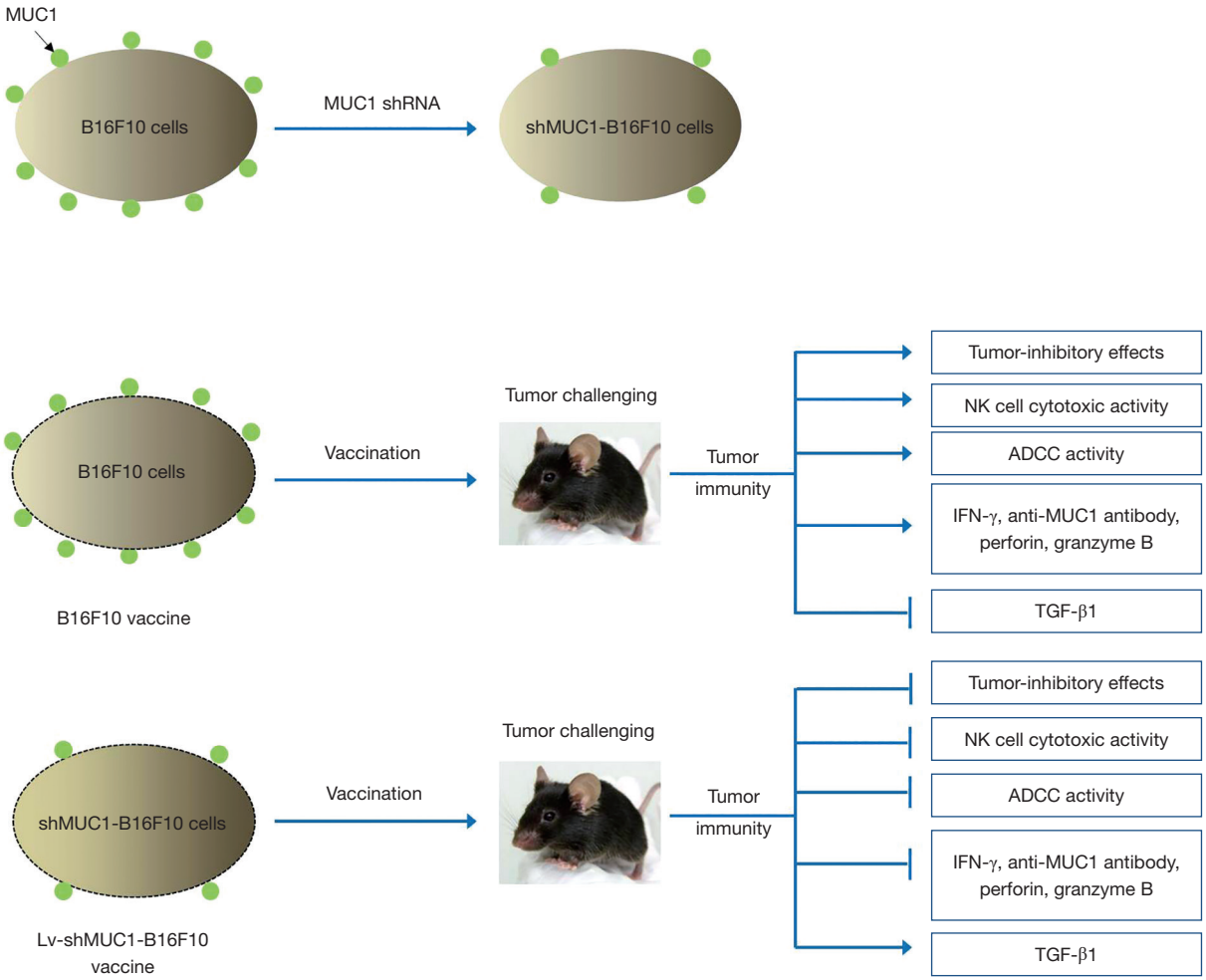

Figure 10 Illustration of MUC1 as a potential candidate for melanoma vaccine development. sh*MUC1* reduced tumor-inhibitory effects, NK cytotoxicity, decreased production of IFN-γ, anti-MUC1 antibodies, *perforin*, *granzyme B*, and elevated TGF-β level induced by B16F10 vaccine. *MUC1*, mucin 1; sh*MUC1*, short hairpin *MUC1*; NK, natural killer; ADCC, antibody dependent cell-mediated cytotoxicity; IFN-γ, interferon-γ; TGF-β1, tumor growth factor-β1.

Discussion

Melanoma is a highly aggressive and metastatic cancer that affects various tissues, including the skin, eyes, nasal cavity, anal tube, rectum, and lymph nodes (14,24). Current treatments for metastatic melanoma are limited due to adverse reactions, drug resistance, and disease recurrence (25). Advances in molecular biology have promoted establishment of immunotherapies for metastatic melanoma treatment, including potential anti-tumor vaccines (26-28). MUC1 was ranked the second among 75 antigen candidates of cancer vaccine in a cancer vaccine program of National Cancer Institute, highlighting MUC1 as a promising anticancer target (29). In recent years, many investigations have been carried out for the therapeutic application of MUC1 in various cancers, such as prostate, colon, and pancreatic malignant tumors (11-14). However, its effects in melanoma are unclear. In this study, the influence of *MUC1* downregulation on B16F10 cells *in vitro*, tumor vaccine effects *in vivo*, as well as the potential underlying mechanisms were explored. A lentivirus vector-based anti-*MUC1* shRNA (sh*MUC1*) was used to transfect HEK 293T cells and the stable knockdown cells (Lv-sh*MUC1*-B16F10) were selected.

MUC1, a high molecular weight glycoprotein secreted by epithelial cells, is a major component of the mucosal surface that lubricates and protects the mucosal epithelium (30).

MUC1 is over-expressed in various cancers, including lung, pancreatic, prostate, ovarian, and colorectal cancer, where it influences key processes like proliferation, apoptosis, invasion, migration, metastasis, and angiogenesis (31). As demonstrated in the previous study, MUC1-C subunit promotes prostate cancer progression and the self-renewal ability of cancer stem cells (32). Moreover, blocking *MUC1* is reported to impair proliferation, vascularization, invasion, and metastatic potential in spontaneous mouse breast cancer (33). *MUC1* silencing in glioblastoma cells induced telomerase suppression and the G1 phase arrest by modulating cell cycle genes and TGF-β signaling (34). *MUC1* is also reported to promote tumor infiltration and metastasis by enhancing the expression of *vimentin*, *N-cadherin*, and *nuclear* β-*catenin*, while suppressing *E-cadherin* expression in cholangiocarcinoma (35). MUC1-C has been shown to induce EMT by activating zinc finger E-Box binding homeobox 1 (*ZEB1*) and nuclear factor-κB (*NF-κB*) p65 signaling (36). Consistent with previous studies, the proliferation and clone-forming potential of B16F10 cells were reduced following *MUC1* downregulation. Furthermore, the ratio of cells in the G0/G1 phase was elevated upon *MUC1* downregulation, indicating cell cycle arrest and reduced cell division. Moreover, the migration ability of Lv-sh*MUC1*-B16F10 cells was influenced by increased *vimentin* and *N-cadherin*, and decreased *E-cadherin* levels. In summary, MUC1 impaired cell cycle progression, proliferation, migration, and the expression of EMT factors in B16F10 cells *in vitro*, indicating that it may have key roles in B16F10 cells (*Figure 10*).

The elevated, non-polar distribution of MUC1 on the tumor cells, as well as its aberrant glycosylation make it a major antigen candidate for the development of tumor vaccines (37). Lots of MUC1-based tumor vaccines have been in research and development, including DNA vaccines, protein vaccines, and glycopeptide vaccines. Furthermore, some of them are under clinical investigation. For example, dendritic cell vaccines containing the MUC1 glycopeptide were used to treat 17 non-metastatic prostate cancer patients, whereas autologous dendritic cells with the MUC1 glycopeptide have been applied in intradermal and intralymphnode dosing (38). The MUC1-based dendritic cell vaccines exhibited safety in patients and elicited significant $CD8^+$ T cell and $CD4^+$ T cell immune responses (39). It has previously been shown that downregulating MUC1 expression in colon cancer stem cells (CCSCs) may damage the immune effects of CCSC vaccines. MUC1 is a multifaceted oncoprotein in the development of cancers. Protein structure analysis revealed that there were 20–120 variable number tandem repeats region abundant of T cell receptor and B cell receptor recognition region in the extracellular domain of MUC1 molecule, which may serve as potential vaccine target (18). Therefore, we thought MUC1 could increase the activation of $CD8^+$ tumor infiltrated lymphocytes and killing effect. To explore if MUC1 is a key antigen in melanoma cells, a tumor vaccine was developed by repeated freeze-thawing of Lv-sh*MUC1*-B16F10 cells and injected it into C57BL/6 mice. The result showed that in mice, the Lv-sh*MUC1*-B16F10 vaccine reduced tumor growth, had a weaker effect against B16F10 cell challenge, and poorer antitumor effects than those of B16F10 and scramble vaccines. Consistent with the previous findings, these results indicated that the immunogenicity and immune effects of the Lv-sh*MUC1*-B16F10 vaccine was attenuated by *MUC1* downregulation (*Figure 10*). Mechanistically, the mice vaccinated with the Lv-sh*MUC1*-B16F10 vaccine exhibited lessened levels of *perforin* and *granzyme B*, reduced NK cell cytotoxicity against YAC-1 cells, and decreased ADCC activity against B16F10 cells when compared with mice inoculated with B16F10 or scramble vaccines. Melanoma cells could be killed by NK cells through secretion of perforin and granzyme B when mice were treated with melanoma vaccines. Perforin can damage the outer membrane of melanoma cells, allowing granzyme B to be released into the cytoplasm of melanoma cells. There, granzyme B triggers an enzyme chain reaction leading to cell apoptosis. Furthermore, NK cells of the mice immunized with the Lv-sh*MUC1*-B16F10 vaccine secreted less IFN-γ and more TGF-β (*Figure 10*). It is known that IFN-γ enhances the immune response by regulating the humoral and cellular immune functions, and has opposite effects of TGF-β on diverse cellular functions that TGF-β regulates a variety of key events in the pathogenesis of diseases including tissue disorders, fibrosis, and cancer, in especial its immunosuppressive role in tumor immunotherapy. Overall, these results indicate that MUC1 acts as a key antigen candidate for the B16F10 cell vaccine.

Conclusions

A melanoma cell vaccine may exert therapeutic effects by inducing immune response *in vivo*. In mice, the MUC1 molecule has high immunogenicity and is a key antigen candidate for melanoma vaccine development,

which provokes strong immune responses that inhibit melanoma growth and enhance survival, whilst the *MUC1* knockdown in B16F10 cell vaccine resulted in reducing the NK cytotoxicity, decreasing the levels of IFN-γ, anti-MUC1 antibody, *perforin*, *granzyme B*, and increased TGF-β level as well as attenuating the anti-melanoma efficacy. These findings highlight MUC1 as an important dominant target antigen and offer novel insights into melanoma vaccine development. However, further research is needed to determine whether upregulating *MUC1* expression in B16F10 cells could improve the tumor-inhibitory activity of the B16F10 vaccine and to uncover its underlying mechanisms. Such studies will offer a reliable experimental basis for the B16F10 cell melanoma vaccine.

Acknowledgments

Funding: This work was supported by the Scientific Research Foundation of Nanjing Health Commission (No. YKK20232), the Natural Science Foundation of Jiangsu Province (No. BK20211169), and the Jiangsu Planned Projects for Postdoctoral Research Funds (No. 2021K518C).

Footnote

Reporting Checklist: The authors have completed the ARRIVE reporting checklist. Available at https://atm.amegroups.com/article/view/10.21037/atm-22-6170/rc

Data Sharing Statement: Available at https://atm.amegroups.com/article/view/10.21037/atm-22-6170/dss

Conflicts of Interest: All authors have completed the ICMJE uniform disclosure form (available at https://atm.amegroups.com/article/view/10.21037/atm-22-6170/coif). The authors have no conflicts of interest to declare.

Ethical Statement: The authors are accountable for all aspects of the work in ensuring that questions related to the accuracy or integrity of any part of the work are appropriately investigated and resolved. Experiments were performed under a project license (No. 20200405010) granted by the animal research and ethics board of Southeast University, in compliance with Chinese Ethics Committee guidelines for the care and use of animals.

References

1. Ahmed B, Qadir MI, Ghafoor S. Malignant Melanoma: Skin Cancer-Diagnosis, Prevention, and Treatment. Crit Rev Eukaryot Gene Expr 2020;30:291-7.
2. Postlewait LM, Farley CR, Seamens AM, et al. Morbidity and Outcomes Following Axillary Lymphadenectomy for Melanoma: Weighing the Risk of Surgery in the Era of MSLT-II. Ann Surg Oncol 2018;25:465-70.
3. Lee N, Zakka LR, Mihm MC Jr, et al. Tumour-infiltrating lymphocytes in melanoma prognosis and cancer immunotherapy. Pathology 2016;48:177-87.
4. Byrne EH, Fisher DE. Immune and molecular correlates in melanoma treated with immune checkpoint blockade. Cancer 2017;123:2143-53.
5. Albittar AA, Alhalabi O, Glitza Oliva IC. Immunotherapy for Melanoma. Adv Exp Med Biol 2020;1244:51-68.
6. Rebecca VW, Sondak VK, Smalley KS. A brief history of melanoma: from mummies to mutations. Melanoma Res 2012;22:114-22.
7. Baars A, van Riel JM, Cuesta MA, et al. Metastasectomy and active specific immunotherapy for a large single melanoma metastasis. Hepatogastroenterology 2002;49:691-3.
8. Guo C, Manjili MH, Subjeck JR, et al. Therapeutic cancer vaccines: past, present, and future. Adv Cancer Res 2013;119:421-75.
9. Zhao F, He X, Sun J, et al. Cancer stem cell vaccine expressing ESAT-6-gpi and IL-21 inhibits melanoma growth and metastases. Am J Transl Res 2015;7:1870-82.
10. Zhao F, Zhang R, Wang J, et al. Effective tumor immunity to melanoma mediated by B16F10 cancer stem cell vaccine. Int Immunopharmacol 2017;52:238-44.
11. Syrkina MS, Rubtsov MA. MUC1 in Cancer Immunotherapy - New Hope or Phantom Menace? Biochemistry (Mosc) 2019;84:773-81.
12. McGuckin MA, Lindén SK, Sutton P, et al. Mucin dynamics and enteric pathogens. Nat Rev Microbiol

2011;9:265-78.
13. Guo M, You C, Dong W, et al. The surface dominant antigen MUC1 is required for colorectal cancer stem cell vaccine to exert anti-tumor efficacy. Biomed Pharmacother 2020;132:110804.
14. Khan H, Makwana V, Santos SND, et al. Development, Characterization, and In Vivo Evaluation of a Novel Aptamer (Anti-MUC1/Y) for Breast Cancer Therapy. Pharmaceutics 2021;13:1239.
15. Kufe DW. MUC1-C in chronic inflammation and carcinogenesis; emergence as a target for cancer treatment. Carcinogenesis 2020;41:1173-83.
16. Zhang Y, Dong X, Bai L, et al. MUC1-induced immunosuppression in colon cancer can be reversed by blocking the PD1/PDL1 signaling pathway. Oncol Lett 2020;20:317.
17. Wang X, Zhao F, Shi F, et al. Reinforcing B16F10/GPI-IL-21 vaccine efficacy against melanoma by injecting mice with shZEB1 plasmid or miR200c agomir. Biomed Pharmacother 2016;80:136-44.
18. Guo M, Luo B, Pan M, et al. MUC1 plays an essential role in tumor immunity of colorectal cancer stem cell vaccine. Int Immunopharmacol 2020;85:106631.
19. Li F, Zhao F, Li M, et al. Decreasing New York esophageal squamous cell carcinoma 1 expression inhibits multiple myeloma growth and osteolytic lesions. J Cell Physiol 2020;235:2183-94.
20. Li M, Pan M, Wang J, et al. miR-7 Reduces Breast Cancer Stem Cell Metastasis via Inhibiting RELA to Decrease ESAM Expression. Mol Ther Oncolytics 2020;18:70-82.
21. Dou J, Ni Y, He X, et al. Decreasing lncRNA HOTAIR expression inhibits human colorectal cancer stem cells. Am J Transl Res 2016;8:98-108.
22. Dou J, Wang Y, Yu F, et al. Protection against Mycobacterium tuberculosis challenge in mice by DNA vaccine Ag85A-ESAT-6-IL-21 priming and BCG boosting. Int J Immunogenet 2012;39:183-90.
23. Sun Y, Liu X, Wang L, et al. High-performance SOD mimetic enzyme Au@Ce for arresting cell cycle and proliferation of acute myeloid leukemia. Bioact Mater 2022;10:117-30.
24. Kanitakis J. Anatomy, histology and immunohistochemistry of normal human skin. Eur J Dermatol 2002;12:390-9; quiz 400-1.
25. da Silveira Nogueira Lima JP, Georgieva M, Haaland B, et al. A systematic review and network meta-analysis of immunotherapy and targeted therapy for advanced melanoma. Cancer Med 2017;6:1143-53.
26. Homet B, Ribas A. New drug targets in metastatic melanoma. J Pathol 2014;232:134-41.
27. Marin-Acevedo JA, Dholaria B, Soyano AE, et al. Next generation of immune checkpoint therapy in cancer: new developments and challenges. J Hematol Oncol 2018;11:39.
28. Amlani A, Barber C, Fifi-Mah A, et al. Successful Treatment of Cytokine Release Syndrome with IL-6 Blockade in a Patient Transitioning from Immune-Checkpoint to MEK/BRAF Inhibition: A Case Report and Review of Literature. Oncologist 2020;25:e1120-3.
29. Cheever MA, Allison JP, Ferris AS, et al. The prioritization of cancer antigens: a national cancer institute pilot project for the acceleration of translational research. Clin Cancer Res 2009;15:5323-37.
30. Apostolopoulos V, McKenzie IF, Pietersz GA. Breast cancer immunotherapy: current status and future prospects. Immunol Cell Biol 1996;74:457-64.
31. Chen W, Zhang Z, Zhang S, et al. MUC1: Structure, Function, and Clinic Application in Epithelial Cancers. Int J Mol Sci 2021;22:6567.
32. Hagiwara M, Yasumizu Y, Yamashita N, et al. MUC1-C Activates the BAF (mSWI/SNF) Complex in Prostate Cancer Stem Cells. Cancer Res 2021;81:1111-22.
33. Merikhian P, Darvishi B, Jalili N, et al. Recombinant nanobody against MUC1 tandem repeats inhibits growth, invasion, metastasis, and vascularization of spontaneous mouse mammary tumors. Mol Oncol 2022;16:485-507.
34. Kim S, Seo Y, Chowdhury T, et al. Inhibition of MUC1 exerts cell-cycle arrest and telomerase suppression in glioblastoma cells. Sci Rep 2020;10:18238.
35. Deng X, Jiang P, Chen J, et al. GATA6 promotes epithelial-mesenchymal transition and metastasis through MUC1/β-catenin pathway in cholangiocarcinoma. Cell Death Dis 2020;11:860.
36. Rajabi H, Kufe D. MUC1-C Oncoprotein Integrates a Program of EMT, Epigenetic Reprogramming and Immune Evasion in Human Carcinomas. Biochim Biophys Acta Rev Cancer 2017;1868:117-22.
37. Panasiuk M, Zimmer K, Czarnota A, et al. Chimeric virus-like particles presenting tumour-associated MUC1 epitope result in high titers of specific IgG antibodies in the presence of squalene oil-in-water adjuvant: towards safe cancer immunotherapy. J Nanobiotechnology 2022;20:160.
38. Scheid E, Major P, Bergeron A, et al. Tn-MUC1 DC Vaccination of Rhesus Macaques and a Phase I/II Trial in

Patients with Nonmetastatic Castrate-Resistant Prostate Cancer. Cancer Immunol Res 2016;4:881-92.
39. Pecher G, Häring A, Kaiser L, et al. Mucin gene (MUC1) transfected dendritic cells as vaccine: results of a phase I/II clinical trial. Cancer Immunol Immunother 2002;51:669-73.

(English Language Editor: J. Jones)

Cite this article as: Shi F, Xue R, Xu H, Mei F, Bao X, Dou J, Zhao F. Mucin 1 downregulation decreases the anti-tumor effects of melanoma vaccine. Ann Transl Med 2022;10(24):1361. doi: 10.21037/atm-22-6170

